Journal of Current Science and Technology, May-August 2021 Vol. 11 No. 2, 311-323
ISSN 2630-0656 (Online)

Cite this article: Jakthreemongkol, P., Pornwongthong, P., Lethaisong, P., Jamparuang, P., Lueangarun, S., & Juntongjin, P. (2021, May). Development and evaluation of "Safe, Affordable, Friendly, and Effective" UVC sterilizer for reusing N95 medical masks. *Journal of Current Science and Technology, 11*(2), 311-323. DOI: 10.14456/jcst.2021.31

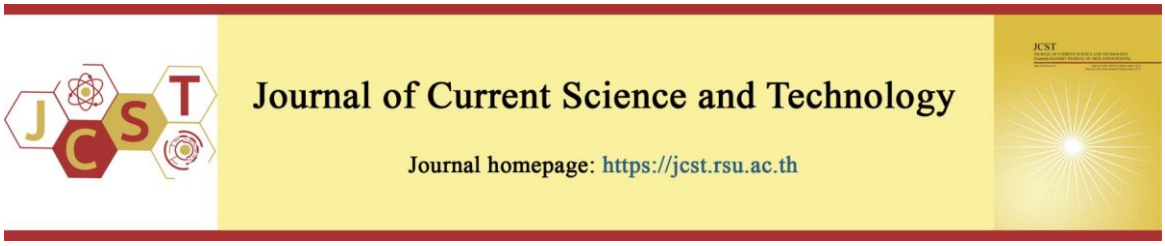

Development and evaluation of "Safe, Affordable, Friendly, and Effective" UVC sterilizer for reusing N95 medical masks

Prasita Jakthreemongkol[1], Peerapong Pornwongthong[2], Phakkhaphum Lethaisong[2], Pollawat Jamparuang[3] Suparuj Lueangarun[1], and Premjit Juntongjin[1]*

[1]Division of Dermatology, Chulabhorn International College of Medicine, Thammasat University, Pathum Thani 12120, Thailand
[2]Scientific Instrument and High-Performance Computing Center, Faculty of Applied Science, King Mongkut's University of Technology North, Bangkok 10800, Thailand
[3]Radiometry Laboratory, Light and Color Group, Thermometry and Optical Metrology Department, National Institute of Metrology, Pathum Thani 12120, Thailand

*Corresponding author, E-mail: premjitvp@yahoo.com

Received 10 February 2021; Revised 28 April 2021; Accepted 7 May 2021;
Published online 27 May 2021

Abstract

Shortage of NIOSH-approved N95 filtering facepiece respirators (FFRs) has made healthcare workers concerned during the COVID-19 pandemic. CDC has recommended ultraviolet germicidal irradiation (UVGI) for medical mask reuse. This study aims to develop UVC germicidal cabinet to sterilize N95 FFRs with four to five log reduction without losing protective properties. UVC germicidal cabinet is fitted with two low-pressure mercury discharge lamps (UVC T8, 40W) at the top and bottom. Radiometric performance tests were conducted and exposure time for decontamination was calculated targeting 1 J·cm^{-2} or 10000 J·m^{-2}. Four samples of 1870 + N95 3M™ were selected to be tested after decontamination. The peak wavelength of UVC light source was 253.89 nm ± 0.60 nm with UVC irradiance value in the range from 6.56 W·m^{-2} at P#9 to 17.9 W·m^{-2} at P#5. The result showed no ozone production from the lamp after one-hour monitoring with ≤ 1 percent instability after six minutes of lamp operation. The calculated time is 564.961 sec or 10 minutes according to maximum UVC irradiance at P#5 (17.9 W·m^{-2}), resulting in UVC dose of 3463.21 J·m^{-2} at minimum UVC irradiance at P#9, which still exceeds D_{90} values. No visible change and unfavorable odor were detected up to 12 cycles. The SEM showed no significant change up to 10 cycles, the distortion and fusion became obvious at cycle 15 and totally damaged at cycle 16, which correlated with the percentage filtration efficiency, which was lower than 95 percent, more specifically, 90.4070 percent at 16 cycle at the maximum point "P#5". This study demonstrated decontamination of N95 FFRs in dose 1 J·cm^{-2} up to 10 cycles without losing properties and recommended placing masks at the center of UVC germicidal cabinet to gain targeted dose. Prospective studies with additional models of N95 FFRs are required and performing strength tests on respiratory coupons and straps is recommended.

Keywords**:** *COVID-19; filtering facepiece respirators (FFRs); N95 medical masks; ultraviolet germicidal irradiation (UVGI); UVC germicidal cabinet; UVC sterilizer.*

1. Introduction

SARS-CoV-2 or COVID-19 is an acute respiratory disease tath originated from the city of Wuhan in the Hubei province of China in December 2019 (Lu et al., 2020). Respiratory aerosols and droplets or contact with the infected secretions can lead to the transmission of SARS-CoV-2 (Letko, Marzi, & Munster, 2020; Li et al., 2020). The N95 respirator has been designed to infiltrate airborne particles, and it can block at least 95 percent of very

small (0.3 micron) test particles. Recently, we found that the actual size of SARS-CoV-2 is of approximately 150 nm while the size of the viral aerosol particles is around 1 µm (Matsuyama et al., 2020). Thus, the filtration efficiency of N95 respirators is considered to be sufficient for personal protection. However, in a study that evaluated the persistence of SARS-CoV-2, showed that the virus that can survive for up to 72 hours on plastic, stainless steel, and cardboard surfaces (van Doremalen et al., 2020). Additionally, Chin et al. (2020) showed that there was a detectable level of infectious virus on the outermost layer of the surgical mask on day seven (Chin et al., 2020).

However, due to the shortage of the N95 respirators, Centers for Disease Control and Prevention (CDC) recommends to reuse filtering facepiece respirators (FFRs), and ultraviolet germicidal irradiation (UVGI) may be the most optimal method to decontaminate and reuse N95 respirators because of the effectiveness and safety of this process. The germicidal effectiveness of UVC peaks at around 260 nm to 265 nm, which correlates with the peak of UV absorption by RNA and DNA material (Kowalski, 2009). The dosage of UVC to disinfect respirator varies in the range proposed by Kowalski, Walsh, and Petraitis (2020), Specifically, the mean of D_{90} values is 308 $J \cdot m^{-2}$, with a wide range of the D_{90} values, that is, 7 $J \cdot m^{-2}$ to 2410 $J \cdot m^{-2}$ (Kowalski, Walsh, & Petraitis, 2020). José G B Derraik (2020) suggested that the least UVC dosage for successful deactivation of SARS-CoV-2 on N95 FFRs would likely be near to 1000 $mJ \cdot cm^{-2}$, as showcased by the study conducted by Heimbuch and Harnish in 2019 (Derraik, Anderson, Connelly, & Anderson, 2020). The UVGI decontamination testing performed by Heimbuch and Harnish in 2019 showed that there are no detectable viable viruses after UV treatment for seven minutes and 15 seconds, thereby resulting in a UV dose of 1 $J \cdot cm^{-2}$ on all soiling conditions, considering no soiling agent, mucin, and sebum with more than 4.81, 3.95, and 4.28 log reductions on SARS-CoV. UVC is absorbed by the outermost layer of corneal epithelium, which can cause a painful transient inflammatory condition—photokeratitis. Additionally, UVC is strongly attenuated by superficial epidermis and causes skin symptoms. The epidermal signs and symptoms such as erythema, tearing, burning sensation, pain, and irritation (Trevisan et al., 2006). The proper use of the UV light, including the warning signs and labels, protective equipment, and symptoms of UV exposure are suggested.

As with most UVC germicidal cabinet on the market today, they tend to be small due to the use of UVC LED lamps. The disadvantage is that it has a low-power output; therefore, it takes a higher time for sterilization as a larger UVC incubator has not been manufactured yet. However, there is no clear research on how masks should be sterilized without compromising their effectiveness when using the UVC germicidal cabinet at present. They are also expensive and it is not possible to manufacture a sterilizer box that is large enough to sterilize large quantities of masks, especially in hospitals.

2. Objectives

To develop a UVC sterilizer box by applying Safety, Affordable, Friendly use, and Effective ("S.A.F.E.") principles to enable the reuse of N95 respirators without loss of its protective efficacy during the COVID-19 pandemic.

3. Materials and methods

3.1 UVC germicidal lamp cabinet

The structure of the UVC germicidal lamp cabinet is composed of cold rolled steel sheet and it is coated with the hybrid powder paint (Epoxy + polyester) inside and outside.

The chamber was fitted with two of the UV-C T8 lamps at the top and bottom, as low-pressure mercury discharge lamps deliver the peak wavelength of 254 nm. The safety door function could operate the system only upon closing, and it would shut down the lamp in a case of an emergency opening. The dimensions of the UVC germicidal cabinet are 730 mm. wide, 304 mm. long, and 400 mm. height when measured from the outside, and the dimensions are 640 mm. wide, 304 mm. long, and 400 mm. height when measured from the inside of the UVC sterilizer cabinet. The operating system is controlled by a digital countdown timer, which can be to set in the range from 1 sec to 9 999 sec. UVC lamps are driven by electronic circuit for low temperature rise, which contributes to a long lifespan up to 8000 hrs. The rated input voltage is in the range from 220 VAC to 240 VAC with 50 or 60 Hz frequency. Total operation power is 40 W, and the operation current is 200 mA. An image of the UVC germicidal cabinet is shown in Figure 1.

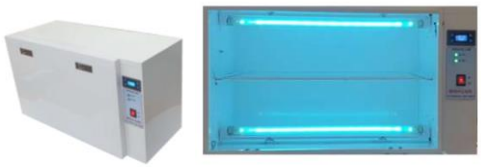

Figure 1 UVC germicidal lamp cabinet fitted with two of the UV-C T8 low-pressure mercury discharge lamps

3.2 Radiometric performance testing

All radiometric performance testing was performed in controlled environmental conditions. The measurement was carried out in an ambient temperature of (23.0 ± 2.0) °C and relative humidity of (50 ± 15) percentage RH (%RH) in the dark room.

3.3 Spectral power distribution and related parameters

The emission spectrum of the UVC source was evaluated while measuring the instability of UVC irradiance using the CAS140CT-154 standard spectrometer of National Institute of Metrology (Thailand), NIMT at the center of the UVC germicidal cabinet.

3.4 Integrated UVC irradiance

The UVC irradiance was measured using a working standard UVC meter of NIMT, which is manufactured by Gigahertz-Optik GmbH, P-9710 (Radiometer) and UV – 3718 (UVC sensor) in the unit of $W \cdot m^{-2}$. The active area in the UVC germicidal cabinet was equally divided into nine sub-areas—P#1, P#2, P#3, P#4, P#5, P#6, P#7, P#8, and P#9, and the UVC irradiance in each sub-area was then recorded. The UVC irradiances were recorded at the center of the position "P#5" and 30 millimeters from the sides of the UVC germicidal cabinet. The UVC sensor was placed in two different ways, that is, facing up and facing down, by placing the UVC sensor at the grille as reference plane. The nine sub-areas of the UVC germicidal cabinet used as measuring positions are depicted in Figure 2.

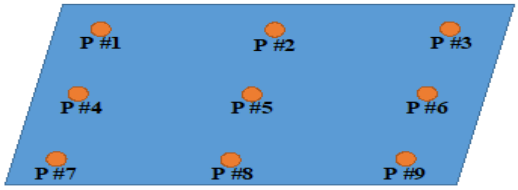

Figure 2 Measuring positions on the reference plane of the UVC germicidal cabinet

3.5 Short-term instability of UVC irradiance

The instability of UVC irradiance was measured with the CAS140CT-154 standard spectrometer of NIMT at the center of the UVC germicidal cabinet for one hour.

3.6 Basic safety testing

3.6.1 UVC leakage

The International Commission on Non-Ionizing Radiation Protection (ICNIRP) exposure limit values UVC effective irradiance at 254 nm, which was measured using a standard UVC meter of NIMT, P-9710 (Radiometer) and UV – 3725 (UVC sensor) in the unit of $W \cdot m^{-2}$ around the UVC germicidal cabinet.

3.6.2 Ozone production

The average ozone concentration was measured using the ozone sensor, SM-EC (0 to 20 ppm) with the ozone monitor, OS-6 from ECO Sensors division of KWJ Engineering Inc., at the center of the UVC cabinet with a one-hour monitoring time. The measurement values helped monitor data through DL-SC3 data viewer and logger software in version 1.0, as provided by the manufacturer.

3.7 Decontamination studies and respirator test

3.7.1 Calculating an exposure time for decontamination of the respirators

According to the findings of the UVGI decontamination testing performed by Heimbuch and Harnish in 2019 (Derraik et al., 2020), the target UVC dose is 1 $J \cdot cm^{-2}$ or 10 000 $J \cdot m^{-2}$, thereby aiming at four to five log reduction (99.99 percent to 99.999 percent reduction) of SARS-CoV. To calculate an exposure time for UVC irradiation, the UVC irradiances, which were measured in nine sub-areas, were selected at maximum of UVC irradiance and minimum of UVC irradiance to calculate the exposure time using a UV dose formula, as shown in Figure 3.

$$H_{e,UVC}=E_{e,UVC} \times t$$

$H_{e,UVC}$ is UVC dose or UVC fluence in the unit of $J \cdot m^{-2}$
$E_{e,UVC}$ *is* UVC irradiance or UVC fluence rate in the unit of $W \cdot m^{-2}$
t is an exposure time in the unit of second

Figure 3 UV dose formula

3.7.2 Screening and selection of N95 filtering facepiece respirators (FFRs)

We randomly selected N95 FFRs, which were currently available in the market during the COVID-19 pandemic. The selected respirator models included 3M™ Aura™ Health Care Particulate Respirator and Surgical Mask 1870+, N95.

The respirator models were tested with, first, scanning electron microscope (SEM) in the mid-side and inside and, second, particle penetration count (percentage filtration efficiency) for evaluating the quality of the masks. All respirators were selected from the same lot number for testing.

3.7.3 Decontamination studies

The respirators were placed on the grille, which is located at the middle of the UVC germicidal cabinet. Two of the respirators were placed at the area of maximum UVC irradiance. One was tested by observational analysis and SEM, whereas another was tested with respect to particle penetration count. The remaining two respirators were placed at the area of minimum UVC irradiance and were tested in the same way as the area of maximum UVC irradiance. Both sides of the test coupon could be exposed to UV irradiation at the grille. In each cycle, after UV decontamination, the FFRs were processed through a respirator test and then returned to decontaminate until the results showed unqualified properties.

3.8 Respirator test

3.8.1 Observational analysis

The control FFR sample and all post-decontamination respirators were inspected for any visible sign of changes or degradation. All samples of FFRs were carefully investigated for any unfavorable odor or smell after the decontamination as well.

3.8.2 Scanning electron microscope (SEM)

The three layers of respiratory coupons were punched from each respirator sample of control FFR and, after UVC exposure, they measured as 5 X 5 mm. in size. Two layers of N95 FFRs are selected for testing by SEM as mid-side and inside. Each individual punched-out respiratory coupon was only tested once after decontamination. SEM images were recorded using a SEM Model QUANTA 450 from FEI.

3.8.3 Particle penetration count and percentage filtration efficiency

SOLAIR 3100 portable airborne particle counters from Lighthouse were used to measure particle penetration for the environment through all the control FFR samples and all post-decontamination respirators. The measurements of particle penetration were recorded as control FFRs, environment (before putting FFRs), and after putting FFRs in each cycle in order to calculate particle filtration efficiency. The formula for calculating particle filtration efficiency is as follows:

$$\%\text{filtration efficiency } (\%)=(a-b)/a$$

a = particle counts environment
b = particle penetration counts of FFRs

4. Results and discussion

4.1 Performance testing result

4.1.1 Spectral power distribution and related parameters

The UV-C lamp that is installed inside the cabinet has a primary emission spectrum in the UV germicidal range. The measured result of peak wavelength is the mean value of 253.89 nm with absolute uncertainty of 0.6 nm.

4.1.2 Integrated UVC irradiance

The UVC irradiances were recorded in nine sub-areas. The maximum of UVC irradiance is 17.9 $W \cdot m^{-2}$ at area P#5 (the center of UVC

germicidal cabinet) and the minimum of UVC irradiance is 6.56 W·m^{-2} at the area P#9. Table 1 shows the values of UVC irradiance in nine sub-areas by placing a UVC sensor in two different way, that is, facing up and facing down.

Table 1 UVC irradiance in nine sub-areas

Positions or direction of sensor	P #1	P #2	P #3	P #4	P #5	P #6	P #7	P #8	P #9
Facing up (W·m^{-2})	8.27	11.3	7.39	13.7	17.9	12.7	7.06	9.69	6.56
Facing down (W·m^{-2})	7.63	10.5	7.04	13.3	17.4	13.5	7.04	9.60	6.72

4.1.3 Short-term instability of UV-C irradiance

The result showed that the unstable UVC irradiance became stable as less than six percent instability after the system was turned on immediately and less than one percent instability after the system was turned on for six minutes, respectively. Thus, the warm-up time of the UVC germicidal cabinet is approximately seven minutes. The instability of UVC irradiance during one-hour monitoring is shown in Figure 4.

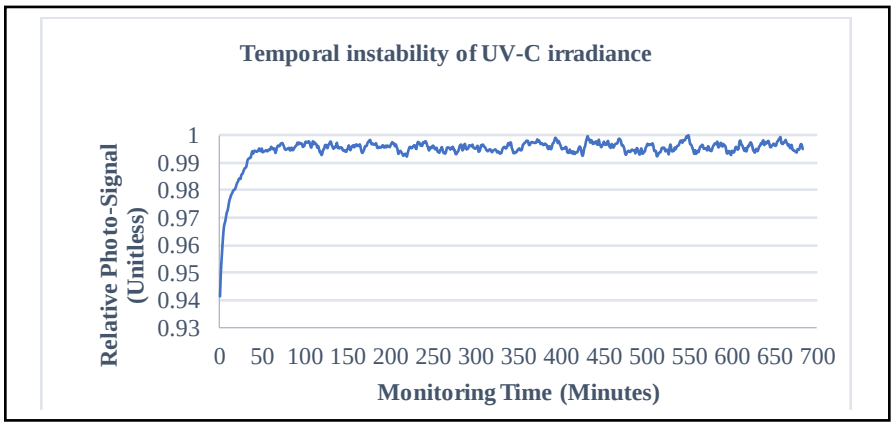

Figure 4 Instability of UV-C irradiance in one-hour monitoring

4.2 Basic safety testing result

4.2.1 UVC leakage

The ICNIRP 254 nm effective irradiance values around the UVC germicidal cabinet have a very low irradiance. The values are various approximately range from 0.003 mW·m^{-2} to 0.005 mW·m^{-2}, which does not exceed the recommended exposure limit (REL) value, as recommended by ICNIRP and NIOSH.

4.2.2 Ozone production

The result *shows* no ozone production within one hour. The average ozone concentration was recorded as 0.00 ppm.

4.3 Decontamination studies and respirator test

4.3.1 Calculating a time for decontamination the respirators

The calculated exposure time at the maximum UVC irradiance position P#5 is 564.961 seconds or approximately 10 minutes, a span during which the targeted UVC dose is 10 000 J·m^{-2}

On the other hand, at the lowest irradiation area at the position "P#9", if the decontamination is done for 10 minutes, then the calculated decontamination dose is a value of 3 463.21 J·m^{-2}, which is still higher than the previously reported dose of D_{90} (Kowalski et al., 2020).

Thus, two respirators were placed into the UVC cabinet at the position "P#5" (maximum UVC irradiance) while two other respirators were placed into the UVC cabinet at the position "P#9" (minimum UVC irradiance) for 10 minutes per cycle.

4.3.2 Decontamination studies

The respirators were placed on the grille, which is located at the middle of the UVC germicidal cabinet. Two respirators were placed at the center of the position "P#5"—the area of

maximum UVC irradiance. Two other respirators were placed at the position "P#9"—the area of minimum UVC irradiance. All the respirators were tested 10 minutes per each cycle with target UVC dose of 1 $J \cdot cm^{-2}$ or 10 000 $J \cdot m^{-2}$.

4.4 Respirator test

4.4.1 Observational analysis

The result showed that there are no physical changes in the material of FFRs during each decontamination cycle up to 12 treatment cycles. After decontamination of all samples of FFRs, neither was any unfavorable odor or smell detectable.

4.4.2 Scanning electron microscope (SEM)

The result showed that SEM images were not significantly changed during each decontamination cycle up to 10 treatment cycles. At cycle 12, the mid-side of respirator models both maximum UVC irradiance position "P#5" and minimum UVC irradiance position "P#9" started getting distorted and fused together. The distortion and fusion of respirator material became obviously totally damaged at cycle 15 and cycle 16.

SEM images of control FFRs before decontamination with UVC of the mid-side and inside of respirator models at magnifications of 100x and 1000x, respectively, are shown in Figure 5.

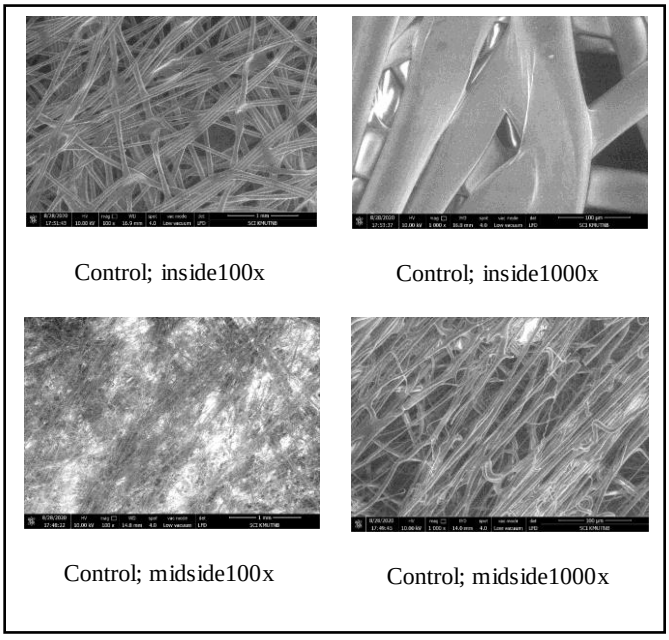

Figure 5 SEM images of two layers; inside and mid-side of the FFRs models of the 3M™ Aura™ Health Care Particulate Respirator and Surgical Mask 1870+ before UVC treatment decontamination at Control; inside100x, inside1000x, midside100x, and midside1000x

The SEM images of inside and mid-side in 100x and 1000x of FFRs models of the 3M™ Aura™ Health Care Particulate Respirator and Surgical Mask 1870+ after UVC treatment decontamination at post UVC decontamination treatment in each cycle, namely cycle 1, 3, 5, 10, 12, 15, and 16, a) at maximum UVC irradiance position "P#5" and b) at minimum UVC irradiance position "P#9" are compared with control, respectively, as shown in Table 2.

Table 2 Comparison of the SEM images of inside 100x and 1000x and mid-side 100x and 1000x of FFRs models of the 3M™ Aura™ Health Care Particulate Respirator and Surgical Mask 1870+ after UVC treatment decontamination at post UVC decontamination treatment in each cycle at maximum UVC irradiance position "P#5" when compared with control and at minimum UVC irradiance position "P#9" when compared with control

	At maximum UVC irradiance position "P#5"				At minimum UVC irradiance position "P#9"			
	inside 100x	inside 1000x	mid-side 100x	mid-side 1000x	inside 100x	inside 1000x	mid-side 100x	mid-side 1000x
Control	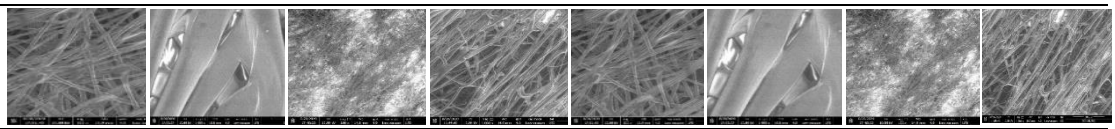							
Cycle-1	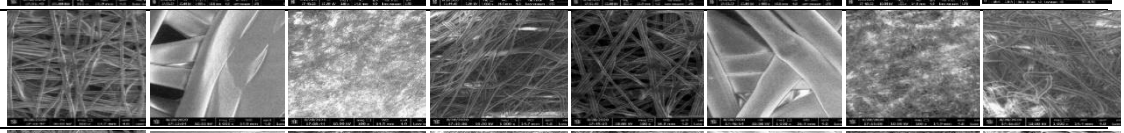							
Cycle-3	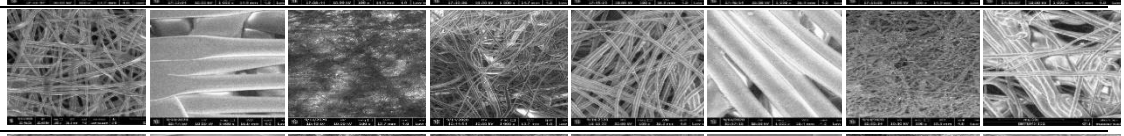							
Cycle-5	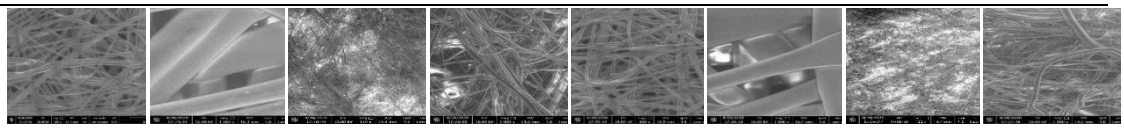							
Cycle-10	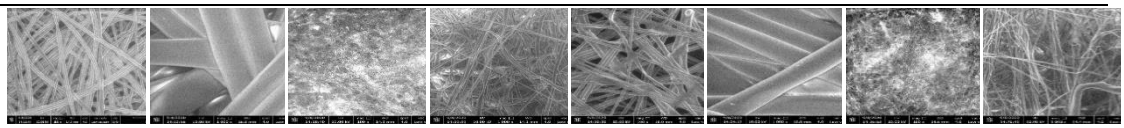							
Cycle-12	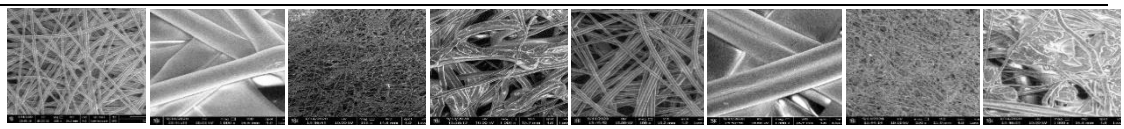							
Cycle-15	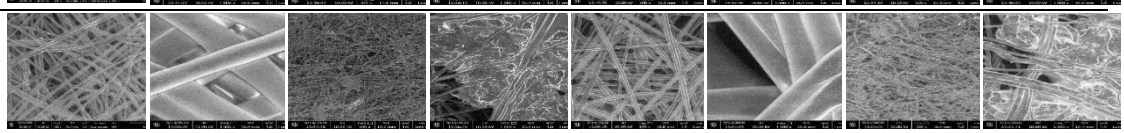							
Cycle-16	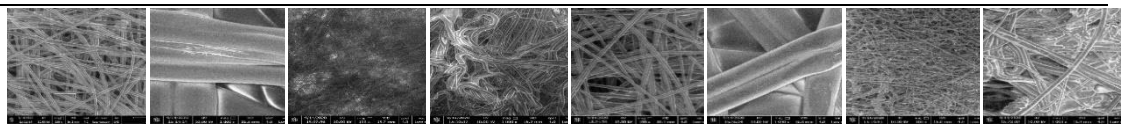							

4.4.3 Particle penetration count and percentage filtration efficiency

Each FFRs model that was decontaminated at maximum point "P#5" and minimum point "P#9" was placed into the SOLAIR 3100 portable airborne particle counters for evaluating particle penetration after decontamination when compared with initial particle penetration of environment with no FFRs in each cycle.

The average three values of initial particle penetration of environment with no FFRs and particle penetration of control FFRs were recorded in Table 3.

Table 3 Summary data of the average three values of initial particle count of environment before placing FFRs, average particle count of control FFRs (no UVC treatment), and calculated percentage filtration efficiency of control FFRs

Control	Average initial particle count of environment before placing FFRs (counts)	Average particle count of control FFRs: No UVC treatment (counts)	Calculated percent filtration efficiency (%)
Control FFRs	1 790 094.00 ± 1.00	29 937.63 ± 302.08	98.327 6 ± 0.016 9

The average three values of initial particle penetration with no FFRs and particle penetration after decontamination in each cycle were recorded at maximum UVC irradiance position "P#5" and at minimum UVC irradiance position "P#9" in Tables 4 and 5, respectively.

Table 4 Summary data of the average three values of initial particle count of environment before placing FFRs, average particle count of FFRs after decontamination at cycle 1, 3, 5, 10, 12, 15, 16, and calculated percentage filtration efficiency of FFRs (after decontamination) at maximum UVC irradiance position "P#5"

Cycle of UVC exposure	Average initial particle count of environment before placing FFRs (counts)	Average particle count of post UVC exposure-max (counts)	Calculated percent filtration efficiency (%)	Percent change of filtration efficiency compared with baseline
Baseline	1 790 094.00 ± 1.00	-	98.327 6 ± 0.016 9	0.00 %
1	1 790 094.00 ± 1.00	32 537.00 ± 1 402.74	98.18 ± 0.08	0.25 %
3	1 406 722 ± 9 544.88	41 740.33 ± 1 938.23	97.03 ± 0.12	1.46 %
5	1 184 886 ± 5 701.01	11 174.00 ± 149.66	99.05 ± 0.01	0.76 %
10	98 026.70 ± 5 600.79	15 286.67 ± 142.03	98.44 ± 0.01	0.14 %
12	1 796 054.00 ± 11 714.90	50 832.67 ± 142.03	97.17 ± 0.05	1.25 %
15	1 823 029.00 ± 2 700.82	66 382.33 ± 194.02	96.36 ± 0.01	2.03 %
16	1 857 353.00 ± 14 467.45	178 175.00 ± 1 750.21	90.41 ± 0.04	8.11 %

Table 5 Summary data of the average three values of initial particle count of environment before placing FFRs, average particle count of FFRs after decontamination at cycle 1, 3, 5, 10, 12, 15, 16, and calculated percentage filtration efficiency of FFRs (after decontamination) at minimum UVC irradiance position “P#9”

Cycle of UVC exposure	Average initial particle count of environment before putting FFRs (counts)	Average particle count of post UVC exposure-min (counts)	Calculated percent filtration efficiency (%)	Percent change of filtration efficiency compared with baseline
Baseline	1 790 094.00 ± 1.00	-	98.327 6 ± 0.016 9	0.00 %
1	1 790 094.00 ± 1.00	34 580.67 ± 932.42	98.07 ± 0.05	0.33 %
3	1 406 722 ± 9 544.88	62 794.67 ± 595.65	95.54 ± 0.07	2.92 %
5	1 184 886 ± 5 701.01	16 052.00 ± 265.89	98.65 ± 0.02	0.37 %
10	98 026.70 ± 5 600.79	22 628.00 ± 2 457.47	97.69 ± 0.26	0.93 %
12	1 796 054.00 ± 11 714.90	37 258.33 ± 615.35	97.93 ± 0.04	0.46 %
15	1 823 029.00 ± 2 700.82	30 420.33 ± 201.46	98.33 ± 0.01	0.03 %
16	1 857 353.00 ± 14 467.45	62 194.33 ± 126.95	96.65 ± 0.03	1.75 %

The post-decontamination FFRs were tested and showed the expected levels of particle filtration efficiency performance. The values of calculated particle filtration efficiency were 98.182 3, 97.032 7, 99.056 9, 98.440 5, 97.169 7, 96.358 7, and 90.407 0 percent at post UVC decontamination treatment cycle 1, 3, 5, 10, 12, 15, and 16 at the at maximum point "P#5" and 98.068 2, 95.536 1, 98.645 3, 97.691 6, 97.925 5, 98.331 3, and 98.331 3 at post UVC decontamination treatment cycle 1, 3, 5, 10, 12, 15, and 16 at the at minimum point "P#9".

The results indicated that percentage filtration efficiency was not affected by UVC decontamination treatment up to 16 cycles at the maximum point "P#5", wherein the level of percentage of particle filtration efficiency was lower than 95 percent (specifically, 90.4070 percent). The summary of calculated percentage filtration efficiency of control FFRs and each cycle after UVC decontamination are shown in Figure 6.

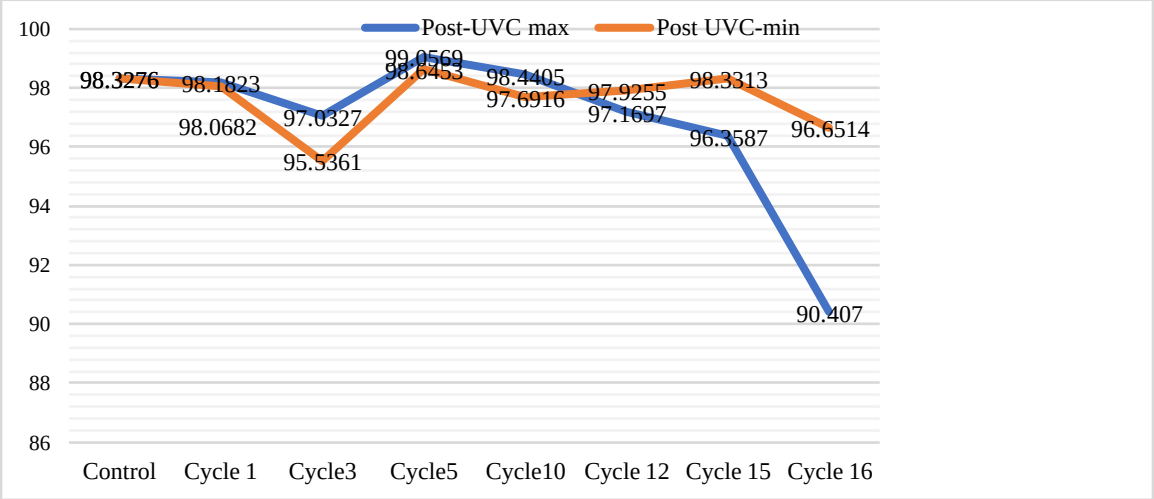

Figure 6 Calculated percentage filtration efficiency of FFRs at control and post UVC decontamination at cycle 1, 3, 5, 10, 12, 15, and 16: Maximum UVC irradiance position “P#5” in blue and minimum UVC irradiance position “P#9” in orange

As there is a shortage of N95 FFRs, which are necessary for use by hospitals and disease screening units, this research was established to produce S.A.F.E. UVC sterilizer boxes while

maintaining safety, affordability, high efficiency, and reliability for sterilizing and reusing medical masks.

The structure of the UVC germicidal lamp cabinet is composed of cold rolled steel sheet and it is coated with the hybrid powder paint (Epoxy + polyester) inside and outside. The chamber is fitted with two of the UV-C T8 lamps as a low-pressure mercury discharge lamp at the top and bottom. The low-pressure mercury discharge lamp was selected, as it emits a main single wavelength at 253.7 nm (254 nm), which intersects the typical DNA absorption curve below the peak absorption (265nm). Nevertheless, the low-pressure mercury discharge lamp has sufficient emission for inactivation of microorganisms, as the strongly absorbed range by nucleic acid is about 250 to 270 nm (Gurzadyan, Gorner, & Schulte-Frohlinde, 1995).

The light distribution is through a uniform-scattered light source that provides a large area of decontamination. The dimensions of the UVC cabinet are 640 mm. wide, 304 mm. long, and 400 mm. height when measured from the inside of the UVC sterilizer cabinet, such that two UVC lamps can cover all the area of the UVC germicidal cabinet. Nevertheless, the efficiency of decontamination depends on the irradiance and fluence (dose) of UVC light, the distance of the light source, and the duration. Therefore, the use of UVC light to ensure the effectiveness of the inactivation of coronaviruses must take into account the factors mentioned above.

The safety door function in the UVC germicidal cabinet can operate only upon closing, and it would shut down the lamp in a case of emergency opening. This is because direct UVC radiation can lead to ocular and skin symptoms. There was reported in 2006 after 26 medical school students were accidentally exposed to UVC radiation for a duration of 90 min. All subjects reported the onset of ocular symptoms and have been diagnosed with photokeratitis along with other skin symptoms (Trevisan et al., 2006). The device has also been tested for basic safety by measuring UVC leakage and ICNIRP effective irradiance value of 254 nm. The result indicated a very low irradiance range from 0.003 $mW \cdot m^{-2}$ to 0.005 $mW \cdot m^{-2}$, which is not higher than the REL, as recommended by ICNIRP or NIOSH. Additionally, the ozone production was tested and showed no ozone production, as shown as 0.00 ppm.

The UVC irradiances of UVC germicidal cabinet vary in each of the nine sub-areas because of the effect of the lamp positioning and the internal reflection. The maximum UVC irradiance is 17.9 $W \cdot m^{-2}$, which is located at area P#5 (the center of UVC cabinet), that is, the nearest to UVC light sources. The reference dose is 1 $J \cdot cm^{-2}$ or 10 000 $J \cdot m^{-2}$ for decontamination (Derraik et al., 2020). The treatment time was calculated to obtain germicidal log reduction between four to five log reductions or 99.999 percent to 99.999 percent, thereby resulting in treatment time of approximately 10 minutes. However, in previous studies, Lindsley et al. (2015) showed a small effect on filtration performance and no effect on flow resistance at doses up to 950 $J \cdot cm^{-2}$ with mean change of penetration $\leq$ 5 percent on N95 FFR models (Lindsley et al., 2015). In addition to the findings of Liao et al. (2020), the result showed slight change of efficiency of melt blown fabric at 10 cycles and drop to ~93 percent at 20 cycles of dwelling time of 600 minutes with 30 $J \cdot cm^{-2}$ UVC dose per cycle (Liao et al., 2020). Thus, the dose of 1 $J \cdot cm^{-2}$ does not tend to affect the filtration efficiency.

It is recommended that N95 FFRs should be placed in the center position, as the UVC irradiance measurement in other positions were found to have different values, ranging from 6.13 $W \cdot m^{-2}$ in the lower right-hand corner (at position P #9 minimum irradiance) to 17.7 $W \cdot m^{-2}$ at center (at position P #5 maximum irradiance). However, at position P #9, the minimum irradiance is still sufficient to facilitate decontamination in D_{90} value or 90 percent reductions with 3463.21 $J \cdot m^{-2}$ (Kowalski et al., 2020).

The SEM images were not significantly changed both inside and mid-side up to 10 treatment cycles. Interestingly, when comparing the calculated percentage filtration efficiency from the number of particle counts, it was found to be in cooperation with the SEM image. The percentage filtration efficiency was slightly reduced in the treatment of 12 cycles (percent change of filtration efficiency when compared with baseline = 1.25 $\%_{max}$, 0.46 $\%_{min}$), whereas the SEM cross-section images started to get distorted and fused together in the mid-side of respirator models, which showed both maximum and minimum UVC irradiance at cycle 12.

Furthermore, percent filtration efficiency was significantly lower than the standard of N95 FFRs at cycle 16—90.407 0 percent at P #5 maximum UVC irradiance (percentage change of filtration efficiency when compared with baseline = 8.11 $\%_{max}$), whereas the distortion and fusion of respirator material became obviously damaged at cycle 15 and totally damaged at cycle 16, respectively.

Nevertheless, the average particle penetration counts after UVC treatment in each cycle does not imply deterioration in the quality of the respirators. As depicted in Figure 7, the fluctuation of particle penetration count values can be responsible for the remaining particles in the environment. The average initial particle count of environment and the average particle count of post UVC exposure in cycle 3, 5, and 10 tended to be low when compared with other cycles. Thus, the calculated percentage filtration efficiency is subject to play a major role to define the function of N95 FFRs. The average initial particle count of environment and particle counts of post UVC exposure in each cycle at P #5 maximum UVC irradiance and P #9 minimum UVC irradiance are shown in Figure 7.

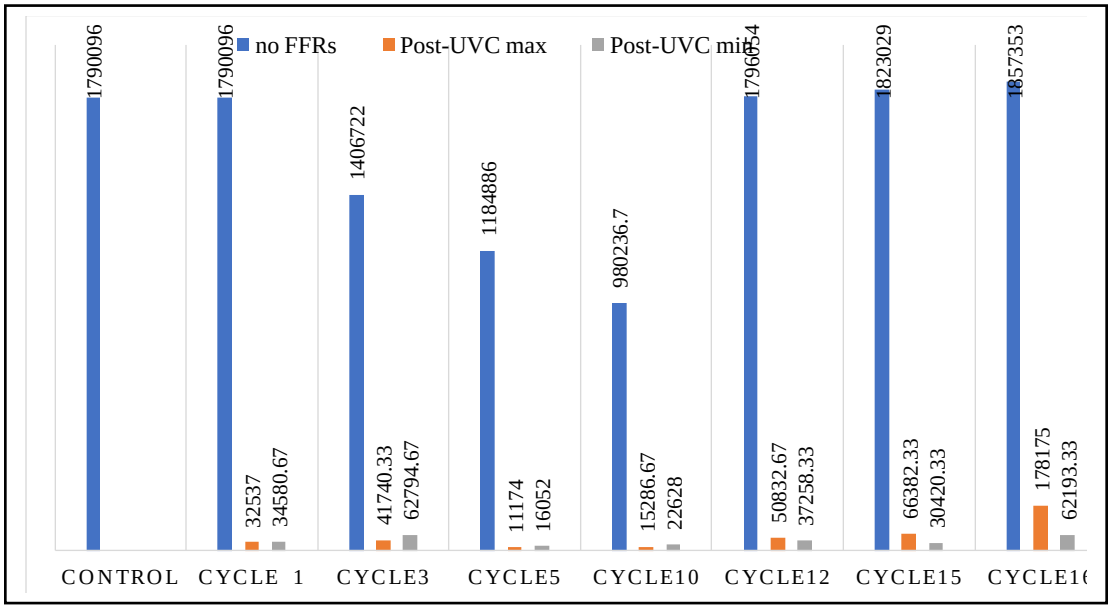

Figure 7 Average initial particle count of environment and post UVC exposure in each cycle

According to the National Institute for Occupational Safety and Health (NIOSH) and CDC recommendations during COVID-19 pandemic regarding the usage guideline of a NIOSH-certified N95 for the protection of healthcare workers, two strategies are recommended, including extended use without decontamination and reuse with decontamination. This is because the outer surfaces of FFRs may become contaminated from exposure to pathogen-laden aerosols. When the wearer accidentally contacts with the FFRs during activities to adjust FFRs or after usage of FFRs, they may contact and be infected with the pathogens on the filter materials. During the COVID-19 pandemic, an effective FFR decontamination method should have the ability to reduce the pathogen burden without losing the aerosol filtration efficiency and maintain the function and breathability of the FFRs while ensuring no visible damage or deformation of FFRs and retain elasticity of straps and no residual chemical hazard. Our study showed that UVGI has been the less time-consuming, safe, and effective way for decontamination of the respirators up to 10 cycles without the loss of properties. However, with regard to these experimental results, various individual parameters are difficult to be controlled with respect to the real-life usage of N95 FFRs. Thus, the aerosol filtration efficiency in this study is possibly better than real-life use because of the stretching, tearing, and deterioration time during the lifetime of use of N95 FFRs. Furthermore, the

elasticity of respirator coupons and straps might be considered after decontamination by UVGI. Nevertheless, a study conducted on the effects of UVGI on N95 respirator filtration performance and structural integrity showed that the strength of straps was less affected by UVGI upon reducing the breaking strength from 20 percent to 51 percent at dose 2 360 $J \cdot cm^{-2}$. Moreover, the bursting strengths of the individual respirator coupon layers showed noticeable decrease at lower doses and it was reduced by 90 percent in some cases at the higher UVGI dose up to 950 $J \cdot cm^{-2}$ (Lindsley et al., 2015). Nevertheless, our study has some limitations—the limited model of N95 FFRs and the limited resources of equipment during the COVID-19 situation. Thus, prospective studies with more models of N95 FFRs need to be conducted and the strength test and the elasticity test of respiratory coupons and straps are recommended to be performed.

5. Conclusion

This study demonstrated the effectiveness of the UVC germicidal cabinet for decontamination, which provides doses up to 1 $J \cdot cm^{-2}$ or 10 000 $J \cdot m^{-2}$ at the center. The calculated exposure time for decontamination of N95 FFRs with target of four to five log reduction (99.99 percent to 99.999 percent reduction) of SARS-CoV is approximately 10 minutes. There are no physical changes or unfavorable odor up to 12 treatment cycles. SEM cross-section images were not significantly changed up to 10 treatment cycles. At cycle 12, the mid-side of respirator models in reference to both maximum and minimum of UVC irradiance started getting distorted and fused together. The distortion and fusion of respirator material became obviously damaged at cycle 15 and totally damaged at cycle 16. However, percentage filtration efficiency was not affected by UVC treatment until 16 cycles at the maximum point "P#5", wherein the particle filtration efficiency was significantly lower than 95 percent, more specifically, 90.407 0 percent, with 8.11 percent change of filtration efficiency when compared with the baseline. The suggestion is to decontaminate N95 FFRs at the center of UVC germicidal cabinet for 10 minutes per cycle and repeating the same up to 10 cycles without losing physical properties, mask structure, and filtration efficiency. Prospective studies with more models of N95 FFRs are suggested, and the strength test and elasticity test of respiratory coupons and straps are recommended.

6. Acknowledgements

This research was granted by Research Gap Fund, National Science and Technology Development Agency (NSTDA) and partially supported by Thammasat University.

7. References

Chin, A., Chu, J., Perera, M., Hui, K., Yen, H.-L., Chan, M., . . . Poon, L. (2020). Stability of SARS-CoV-2 in different environmental conditions. *The Lancet Microbe, 1*(1), e10. DOI: 10.1016/S2666-5247(20)30003-3

Derraik, J. G. B., Anderson, W. A., Connelly, E. A., & Anderson, Y. C. (2020). Rapid evidence summary on SARS-CoV-2 survivorship and disinfection, and a reusable PPE protocol using a double-hit process. *International Journal of Environmental Research and Public Health 17*(17), 6117. DOI: https://doi.org/10.3390/ijerph17176117

Gurzadyan, G. G., Gorner, H., & Schulte-Frohlinde, D. (1995). Ultraviolet (193, 216 and 254 nm) photoinactivation of Escherichia coli strains with different repair deficiencies. *Radiation Research, 141*(3), 244-251. DOI: 10.2307/3579001

Kowalski, W. (2009). *UV Surface Disinfection*. In: Ultraviolet Germicidal Irradiation Handbook. Springer, Berlin, Heidelberg. DOI: https://doi.org/10.1007/978-3-642-01999-9_10

Kowalski, W., Walsh, T., & Petraitis, V. (2020). *2020 COVID-19 Coronavirus ultraviolet susceptibility*. *Technical Report*, Report number: COVID-19_UV_V20200312, Project: UV Disinfection. https://www.researchgate.net/publication/339887436_2020_COVID-19_Coronavirus_Ultraviolet_Susceptibility

Letko, M., Marzi, A., & Munster, V. (2020). Functional assessment of cell entry and receptor usage for SARS-CoV-2 and other lineage B betacoronaviruses. *Nature Microbiology, 5*(4), 562-569. DOI: 10.1038/s41564-020-0688-y

Li, Q., Guan, X., Wu, P., Wang, X., Zhou, L., Tong, Y., . . . Feng, Z. (2020). Early transmission dynamics in Wuhan, China, of novel Coronavirus-infected pneumonia. *New England Journal of Medicine, 382*(13), 1199-1207. DOI: 10.1056/NEJMoa2001316

Liao, L., Xiao, W., Zhao, M., Yu, X., Wang, H., Wang, Q., . . . Cui, Y. (2020). Can N95 respirators be reused after disinfection? How Many Times? *ACS Nano, 14*(5), 6348-6356. DOI: 10.1021/acsnano.0c03597

Lindsley, W. G., Martin, S. B., Jr., Thewlis, R. E., Sarkisian, K., Nwoko, J. O., Mead, K. R., & Noti, J. D. (2015). Effects of ultraviolet germicidal irradiation (UVGI) on N95 respirator filtration performance and structural integrity. *Journal of Occupational and Environmental Hygiene, 12*(8), 509-517. DOI: 10.1080/15459624.2015.1018518

Lu, R., Zhao, X., Li, J., Niu, P., Yang, B., Wu, H., . . . Tan, W. (2020). Genomic characterisation and epidemiology of 2019 novel coronavirus: implications for virus origins and receptor binding. *Lancet, 395*(10224), 565-574. DOI: 10.1016/S0140-6736(20)30251-8

Matsuyama, S., Nao, N., Shirato, K., Kawase, M., Saito, S., Takayama, I., . . . Takeda, M. (2020). Enhanced isolation of SARS-CoV-2 by TMPRSS2-expressing cells. *Proceedings of the National Academy of Sciences of the United States of America, 117*(13), 7001-7003. DOI: 10.1073/pnas.2002589117

Trevisan, A., Piovesan, S., Leonardi, A., Bertocco, M., Nicolosi, P., Pelizzo, M. G., & Angelini, A. (2006). Unusual high exposure to ultraviolet-C radiation. *Photochemistry and Photobiology, 82*(4), 1077-1079. DOI: 10.1562/2005-10-27-ra-728

van Doremalen, N., Bushmaker, T., Morris, D., Holbrook, M., Gamble, A., Williamson, B., . . . Munster, V. (2020). Aerosol and surface stability of SARS-CoV-2 as compared with SARS-CoV-1. *New England Journal of Medicine, 382*. DOI: 10.1056/NEJMc2004973